Design and performance of a composite Tm:YAG laser pumped by VBG-stabilized narrow-band laser diode*

Shu-Tao Dai(戴殊韬)[1,2], Jian-Hong Huang(黄见洪)[1], Hai-Zhou Huang(黄海舟)[1,2], Li-Xia Wu(吴丽霞)[1], Jin-Hui Li(李锦辉)[1], Jing Deng(邓晶)[1], Yan Ge(葛燕)[1], and Wen-Xiong Lin(林文雄)[1,†]

[1] *Key Laboratory of Optoelectronic Materials Chemistry and Physics, Fujian Institute of Research on the Structure of Matter, Chinese Academy of Sciences, Fuzhou* 350002, *China*

[2] *University of Chinese Academy of Sciences, Beijing* 100049, *China*

(Received 16 February 2017; revised manuscript received 18 March 2017; published online 6 June 2017)

A 2-μm composite Tm:YAG laser pumped with a narrow-band laser diode was presented. The temperature distribution and thermal lens in the Tm:YAG were numerically simulated by a finite element method and the results were used to design the special cavity, in order to achieve a high efficiency and stable output. With a 25-W incident pump power, we obtained a maximum output power of 11 W at 2018.5 nm, corresponding to a slope efficiency of 51.3% and an optical-to-optical efficiency of 44.5%, respectively. The beam quality was measured to be $M_x^2 = 1.8$ and $M_y^2 = 1.6$.

Keywords: Tm:YAG, 2 μm laser, thermal effects, diode-pumped

PACS: 42.55.Xi, 42.72.Ai, 42.60.Da, 42.60.By **DOI:** 10.1088/1674-1056/26/7/074211

1. Introduction

Diode-end-pumped solid-state eye-safe 2-μm lasers are of great interest due to their potential applications in coherent Doppler wind lidar and remote sensing,[1–3] and 2-μm lasers are also an ideal pumping laser source for optical parametric oscillators (OPO) and optical parametric amplifiers (OPA) in the mid-infrared wavelength region.[4,5]

Among the laser materials used to generate 2-μm laser emissions, Tm-doped lasers have the ability to use AlGaAs diodes around 800 nm as the pump source while maintaining a high efficiency and low thermal loading.[6] Thus, substantial studies have been dedicated to these laser systems in recent years.[7–10]

However, the characteristics of the small stimulated emission cross sections ($\sim 5 \times 10^{-21}$ cm^2) and quasi-three-level energy levels of the Tm:laser at room temperature require a high pumping intensity for efficient laser operation. The intense pumping power plus the large quantum defect (from 785 nm to 2 μm) will highly deplete the population inversion and generate more heat, and finally results in an increase in the threshold and a decrease in the slope efficiency.[11]

In 2008, Wu *et al.* reported a 6.97 W diode-end-pumped composite Tm:YAG laser at room temperature with a slope efficiency of 41.45%.[12] In 2009, Cheng *et al.* introduced the Tm:YAG ceramic as a gain medium.[13] They obtained a 4.5 W output power with a sloping efficiency of 20.5%. In addition, in 2012, Gao *et al.* increased the slope efficiency to 65% with a maximum output power of 6.05 W.[14] However, the operating temperature was maintained at 281 K, and we could see an obvious saturation at the maximum output. In 2015, Li *et al.* investigated the output characteristics of the Tm:YAG laser in the wide temperature range of 25–300 K.[15] The laser crystal was cooled with a liquid helium cooling system. At the temperature of 88 K, a maximum output power of 4.68 W was achieved with a slope efficiency of 56.1%. However, at the room temperature of 300 K, the output power was decreased to 1.2 W.

In this letter, we developed a high efficiency laser diode (LD) end-pumped composite Tm:YAG laser at room temperature. The LD was wavelength-locked by VBGs at 784.9 nm with a 0.1 nm linewidth. First, the temperature distribution in the laser crystal was numerically simulated using a finite element method. Then we obtained the thermal focal length by calculating the optical path difference of the crystal. Based on the above theoretical calculations, a simple two-mirror compact thermal stability cavity was designed and experimentally tested. Finally, we obtained a maximum output power of 11 W at 2018 nm under the incident pump power of 25 W corresponding to a slope efficiency of 51.3% and an optical-to-optical efficiency of 44.5%, respectively. In addition, the output power is scalable to a considerably higher value with a higher pumping power.

2. Experiment design and setup

The geometry of the composite crystal is shown in Fig. 1. The gain medium was a 3.5 at.% Tm:YAG with dimensions of 3×3×17 mm^3. An undoped YAG with dimensions of 3×3×2 mm^3 was diffusion bonded to one end-face of the active crystal. The composite Tm:YAG was wrapped with in-

*Project supported by the Science and Technology Major Project of Fujian Province, China (Grant No. 2013HZ0003-2).

†Corresponding author. E-mail: wxlin@fjirsm.ac.cn

© 2017 Chinese Physical Society and IOP Publishing Ltd

dium foil and mounted in a water cooled copper sink, which was maintained at 288 K. The pump beam waist was collimated on the facet of the doped portions with two convex lens pairs. The Tm:YAG was one end-pumped by fiber coupled laser diode (LD). The excitation spectrum peak of the laser medium was located at around 785 nm, measured by a fluorescence spectrometer (FSP920, Edinburgh Instruments). Thus, the LD was chosen with a center emission wavelength of 784.9 nm (293 K). A Volume Bragg Grating (VBG) was used to lock its wavelength with a linewidth of 0.1 nm (MIF4S22-785.0, DILAS). The LD had a maximum 24 W output power with a core diameter of 400 μm and numerical aperture (NA) of 0.22.

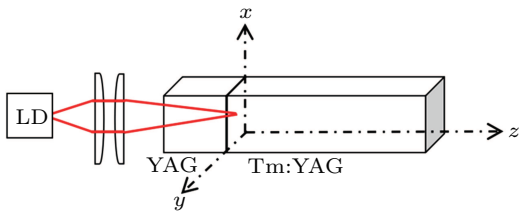


Fig. 1. (color online) Schematic diagram of the end-pumped Tm:YAG/YAG composite crystal.

The thermal effect of the laser medium depends mainly on the heat flux induced by the pump power. In this case, the heat conduction equation describing the temperature distribution in the laser crystal is shown as follows:[16,17]

$$K_x\frac{\partial^2 T(x,y,z)}{\partial x^2}+K_y\frac{\partial^2 T(x,y,z)}{\partial y^2}+K_z\frac{\partial^2 T(x,y,z)}{\partial z^2}+q(x,y,z)=0, \quad (1)$$

where K_x, K_y, K_z are the heat conductivity coefficients along x, y, and z directions respectively; T is the temperature. The heat flux $q(x,y,z)$ can be written as

$$q(x,y,z)=\frac{\eta\alpha P_{\rm in}}{A_0}\exp\left(-\frac{2(x^2+y^2)^2}{\omega_{\rm p}^4(z)}\right)\times\exp[-\alpha(z-{\rm d}l)], \quad (2)$$

where $P_{\rm in}$ is the incident pump power; α is the absorption coefficient; η is the heat generating coefficient due to the quantum defect; ${\rm d}l$ is the undoped YAG crystal length; ω is the radius of the pump light in the laser crystal; A_0 is the pumping area. Here, we supposed the LD intensity has a fourth-order super-Gaussian profile along the x, y-direction.

Considering that the thermal conductivity of the heat sink is much greater than that of the laser crystal, the temperature at the surrounding surfaces of the laser crystal is supposed to be the same as cooling water temperature at 288 K, and the end surfaces are supposed to be adiabatic.

Then, we numerically solve Eq. (1) using a finite element method. Figure 2 shows the simulated two-dimensional temperature distribution along the optical axis at a pumping power of 25 W. The values of the simulation parameters used are $K_x=K_y=K_z=0.5\times10^{-4}$ W·cm^{-1}·K^{-1}, $\eta=0.6$, and $\alpha=2.43$ cm^{-1} (at 3.5 at.% Tm:YAG). Figure 3 shows the thermal distribution of the composite crystal compared with a conventional crystal. The highest temperatures in the Tm:YAG/YAG composite crystal and Tm:YAG are 368 and 388 K, respectively. The highest temperature appeared in the interior for the composite crystal while at the pump facet for the conventional crystal. The Tm:YAG/YAG composite crystal restrained the thermal deformation remarkably. Thus, undoped YAG bonded to Tm:YAG is obviously shown to be an effective method to relieve the thermal effect.

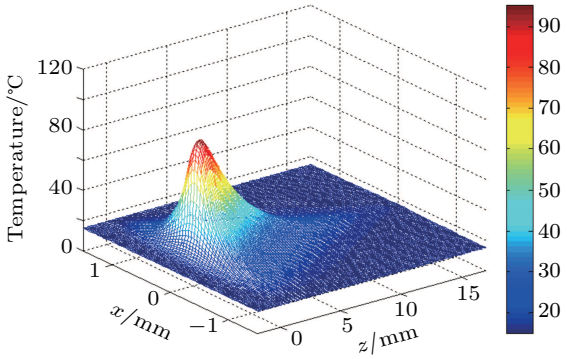


Fig. 2. (color online) The temperature distribution along the crystal z axis at pump power of 25 W.

The gradient distribution of the temperature in crystal results in the temperature-dependent variation of the refractive index and the stress-dependent variation of the refractive index.[18] Therefore, the optical path difference (OPD) for one pass can be expressed as

$${\rm OPD}(x,y)=\int_0^l\left[\frac{{\rm d}n}{{\rm d}T}+n_0(1+\mu)\alpha_{\rm T}\right]\Delta T(x,y,z)\,{\rm d}z, \quad (3)$$

where n and n_0 are the refractive indices of the crystal at the temperature T and at room temperature, respectively; $\alpha_{\rm T}$ is the thermal expansion coefficient; μ is the Poisson's ratio. The values of these parameters are $\alpha_{\rm T}=8.2\times10^{-6}$ °C^{-1}, $\mu=0.6$, and ${\rm d}n/{\rm d}T=7.3\times10^{-6}$ °C^{-1}.

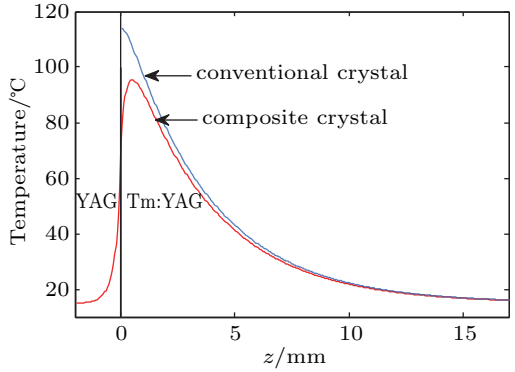


Fig. 3. (color online) The thermal distribution of the composite crystal and conventional crystal.

Figure 4 shows the OPD distribution in the Tm:YAG/YAG crystal at the incident pump powers of 10 W, 20 W, and 25 W. The maximum OPDs at the center of the crystal are 5.9 μm, 9.8 μm, and 13.8 μm, respectively.

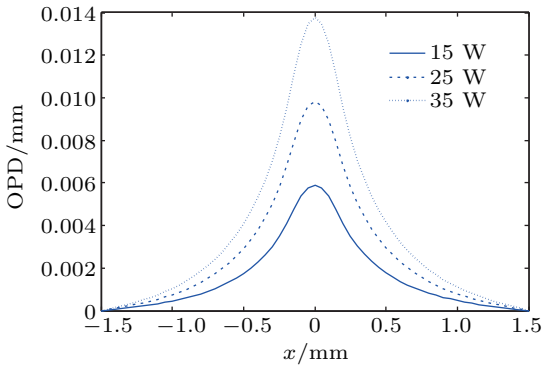


Fig. 4. (color online) The OPD in Tm:YAG/YAG crystal at different pump power.

In the pumped region, it is common to consider the laser crystal to be a thermally induced thin lens. Then, the OPD can be approximated by a quadratic polynomial, and the focal length of the thermally induced lens can be derived by fitting the OPD distribution curve. Figure 5 shows the results of the calculations.

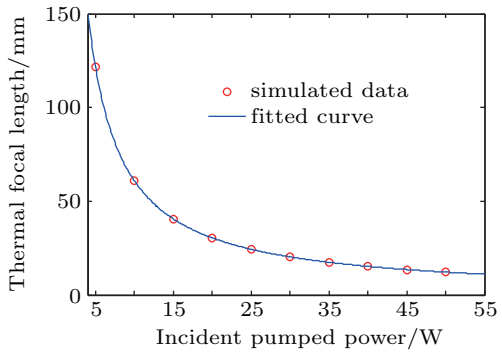


Fig. 5. (color online) The focal length of thermal lens versus pump power.

The experiment setup was shown in Fig. 6. The laser system was similar to that developed by Huang *et al.*[19] The cavity parameters were specifically designed for thermal stability based on the ABCD matrix simulation.[20] M1 was the 45° dichroic mirror that had a high transmission at 785 nm and high reflectivity at 2 μm. M2 was a rear-coated mirror with a high reflectivity at 2 μm and high transmission at 785 nm. M3 was an output coupler with a transmission of 3% at 2 μm. The L-shape cavity was adopted to suppress back reflection of the pump light and to eliminate the influence of residual pump light on the experiment.

Considering the thermal lens effect, we calculate the TEM_{00} cavity mode waist in the crystal center and in the output coupler as a function of the pump power with different cavity lengths, as shown in Fig. 7. Thus, for a plane–plane cavity, the shorter the cavity is, the larger the pump power that can be achieved. The whole resonator length was chosen to be as short as 40 mm, which was limited by mechanical mounts. If the cavity length was much longer or pumping power was much higher, other thermal lens compensation methods should be taken into account.

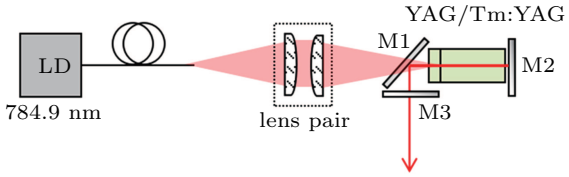


Fig. 6. (color online) The experiment setup.

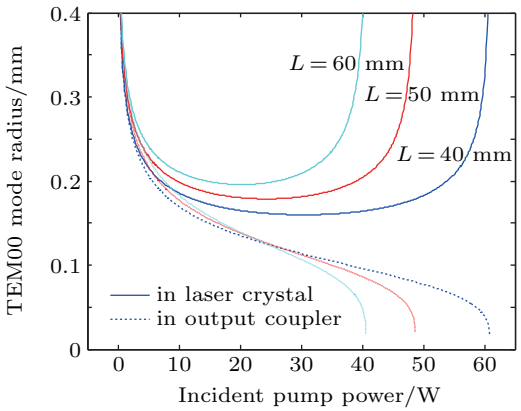


Fig. 7. (color online) Radius of the TEM00 spot versus pump power.

3. Results and discussion

The average 2 μm output power versus the total incident pump power is shown in Fig. 8. The output power increased linearly with the increasing pump power and no saturation effect was observed. A maximum output power of 11.1 W was obtained with an incident pump power of 25 W (with an absorbed pump power of 24.6 W).

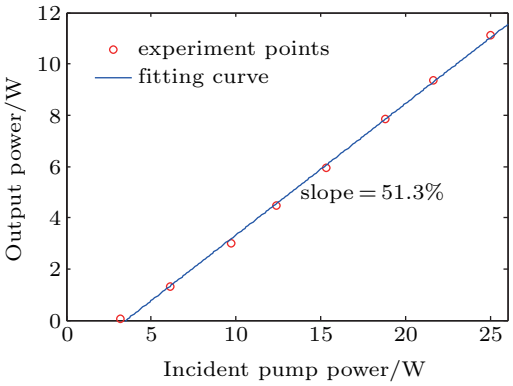


Fig. 8. (color online) Output power versus pump power.

As with the results shown in Fig. 7, when the pump power rises even to 50 W, the TEM_{00} mode radius remains at about 160–180 μm, mode-matched to the pump spot waist

of 200 μm. That is to say, for a pump power between 10 and 50 W, the resonator will be stable and the laser will be in the TEM_{00} mode. We can predict a higher output power maintaining the same slope efficiency with a much higher pump power. Meanwhile, the slope efficiency and optical-to-optical efficiency relative to the absorbed pump power were 52.2% and 45.1%, respectively, and relative to incident pump power were 51.3% and 44.5%, respectively.

The absorbed power was 98.4% of the total incident pump power corresponding to the absorption coefficient of 2.43 cm^{-1} in a 3 at.% doped Tm:YAG crystal at a temperature of 288 K. This high absorption was probably due to the wavelength-locked 784.9 nm LD with a linewidth of 0.1 nm, which matched the excitation band of the Tm:YAG at about 785 nm. Comparing this work with Ju's work,[21] he presented a composite Tm:YAG laser which matched well with our experiment setup. A 42.8% slope efficiency and 33.7% optical conversion efficiency were achieved. The conversion efficiency when pumped with a VBG-stabilized narrow-band LD was much higher than when pumped with a conventional broad-band LD.

At an output power of 11 W, the beam quality factors measured by the beam analyser (NanoModeScan) were $M_x^2 = 1.8$ and $M_y^2 = 1.6$. The laser spectrum at the same output power was centred at 2018.5 nm with a FWHM linewidth of 2.7 nm, measured by an infrared spectrum analyzer (721-IR, Bristol).

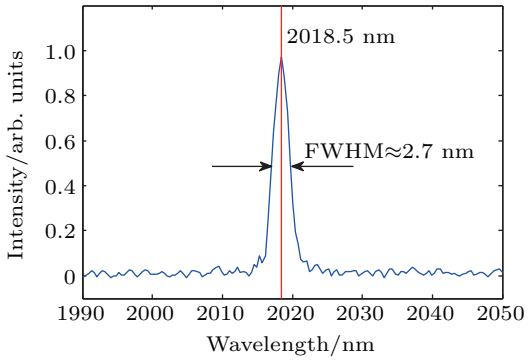


Fig. 9. (color online) Output spectrum at output power of 11.12 W.

4. Conclusion

In summary, we have demonstrated a high-efficiency end-pumped 2-μm Tm:YAG laser. The thermal effects in the Tm:YAG/YAG composite crystal are comprehensively investigated, and the analysed results are used to design the cavity of the laser. Finally, a maximum output power of 11.1 W was obtained with an incident pump power of 25 W. The slope efficiency and optical-to-optical efficiency were 52.2% and 45.1%, respectively, relative to the absorbed pump power, and were 51.3% and 44.5%, respectively, relative to incident pump power. The conversion efficiency, when pumped with a VBG-stabilized narrow-band LD, was significantly higher than when pumped with a conventional broad-band LD. The beam quality factors were $M_x^2 = 1.8$ and $M_y^2 = 1.6$. A higher output power maintaining the high efficiency can be achieved with a higher LD power.

References

[1] Ishii S, Mizutani K, Fukuoka H, Ishikawa T, Philippe B, Iwai H, Aoki T, Itabe T, Sato A and Asai K 2010 *Appl. Opt.* **49** 1809
[2] Kavaya M J, Beyon J Y, Koch G J, Petros K M, Petzar P J, Singh U N, Trieu B C and Yu J 2014 *J. Atmos. Ocean. Tech.* **31** 826
[3] Koch G J, Beyon J Y, Cowen L J, Kavaya M J and Grant M S 2014 *J. Appl. Remote Sensing* **8** 083662
[4] Creeden D, Ketteridge P A, Budni P A, Setzler S D, Young Y E, McCarthy J C, Zawilski K, Schunemann P G, Pollak T M, Chicklis E P and Jiang M 2008 *Opt. Lett.* **33** 315
[5] Gebhardt M, Gaida C, Kadwani P Sincore A, Gehlich N, Jeon C, Shah L and Richardson M 2014 *Opt. Lett.* **39** 1212
[6] Honea E C, Beach R J, Sutton S B, Speth J A, Mitchell S C, Skidmore J A, Emanuel M A and Payne S A 1997 *IEEE J. Quantum Electron.* **33** 1592
[7] Zhang W X, Pan Y B, Zhou J, Liu W B, Li J, Jiang B X, Cheng X J and Xu J Q 2009 *J. Am. Ceram. Soc.* **92** 2434
[8] Wu Q F, Yu L X, Dai T Y, Chen F, Yao B Q, Ju Y L and Wang Y Z 2012 *Laser Phys.* **22** 892
[9] Zhan M J, Zou Y W, Lin Q F, Wang Z H, Han H N, Lu L, Wei Z Y, Zhang J and Tang D Y 2014 *Acta Phys. Sin.* **63** 014205 (in Chinese)
[10] Jin L, Liu P, Liu X, Huang H, Yao W and Shen D 2016 *Opt. Comm.* **372** 241
[11] Li C, Song J, Shen D, Kim N S, Ueda K, Huo Y, He S and Cao Y 1999 *Opt. Exp.* **4** 12
[12] Wu C, Ju Y, Li Y, Wang Z and Wang Y 2008 *Chin. Opt. Lett.* **6** 594
[13] Cheng X J, Xu J Q, Zhang W X, Jiang B X and Pan Y B 2009 *Chin. Phys. Lett.* **26** 074204
[14] Gao W L, Ma J, Xie G Q, Zhang J, Luo D W, Yang H, Tang D Y, Ma J, Yuan P and Qian L J 2012 *Opt. Lett.* **37** 1076
[15] Li J, Yan T, Liang J and Cai J 2015 *Opt. Comm.* **334** 118
[16] Liu Q X and Zhong M 2010 *Acta Phys. Sin.* **59** 8535 (in Chinese)
[17] Zhou Y, Dai Y, Yao S N, Liu J, Chen J B, Chen S F and Xin J G 2013 *Acta Phys. Sin.* **62** 024210 (in Chinese)
[18] Koechner W 2006 *Solid-state Laser Engineering*, 6 edn. (New York: Spriner) p. 444
[19] Huang H Z, Huang J H, Liu H G, Dai S T, Weng W, Zheng H, Ge Y, Li J H, Deng J and Lin W X 2016 *Laser Phys. Lett.* **13** 095001
[20] Milonni P W and Eberly J H 2010 *Laser Physics*, 6 edn. (Hoboken: Wiley) p. 288
[21] Ju Y L, Wu C T, Wang Z G, Li Y F and Wang Y Z 2008 *Laser Phys.* **18** 1316